

**COMPARISON BETWEEN 3D TOF MAGNETIC
RESONANCE ANGIOGRAPHY AND INTRA-
ARTERIAL DIGITAL SUBTRACTION
ANGIOGRAPHY IN IMAGING THE CIRCLE OF
WILLIS**

By

DR ROZITA BT MOHD GHAZALI

Dissertation Submitted In Partial Fulfilment
Of The Requirement For
The Degree of Master Of Medicine (Radiology)



**UNIVERSITI SAINS MALAYSIA
2002**

This dissertation is dedicated to my wonderful parents, Puan Umi Kalsum and Encik Mohd Ghazali who have been my source of inspiration and have supported me throughout the 4 years of my studies. To my husband, Roslan, thank you for your encouragement and understanding.

ACKNOWLEDGMENTS

I would like to express my sincerest gratitude to Associate Professor Dr Ibrahim Lutfi Shuaib, my supervisor, for spending his valuable time to see to the completion of this dissertation. He has been very kind in providing expert assistance in becoming one of the two observers in this study in addition to his guidance and valuable comments throughout the whole duration of this dissertation.

I am also grateful to Dr Syed Hatim from the Department of Community Medicine who has spent time from his busy schedule in providing guidance with the statistical aspect of this dissertation.

Last but not least, I would also like to thank all the lectures, my colleagues and the staffs of the Radiology Department in Hospital Universiti Sains Malaysia who has helped me one way or another in the progression of this dissertation.

TABLE OF CONTENT

<i>Acknowledgements</i>	<i>ii</i>
<i>Table of contents</i>	<i>iii</i>
<i>List of tables</i>	<i>v</i>
<i>List of figures</i>	<i>vii</i>
<i>Abbreviations</i>	<i>ix</i>
<i>Abstract</i>	
<i>Bahasa Melayu</i>	<i>x</i>
<i>English</i>	<i>xii</i>
Chapter 1: Introduction and Literature Review	
1.1 Introduction	1
1.2 Magnetic resonance angiography	
1.2.1 Basic concept	2
1.2.2 MR parameters and methods important in MR acquisitions	5
1.2.3 Limitations of TOF	8
1.2.4 Post processing of an MRA	9
1.2.5 Applications of intracranial 3D TOF MRA	10
1.3 Anatomic evaluation of the circle of Willis	15

Chapter 2: Aim and objectives	
2.1 Aim	21
2.2 Objectives	21
2.3 Null hypothesis	22
Chapter 3: Methodology	23
3.1 Imaging modalities	24
3.2 Image analysis	26
3.2.1 3D TOF MRA technique	27
3.2.2 IADSA technique	28
3.3 Data and statistical analysis	29
Chapter 4: Results	34
Chapter 5: Discussion	59
Chapter 6: Summary, conclusion and recommendation	68
Chapter 7: References	70

LIST OF TABLES

Table 3.1	Measurements of the accuracy of a diagnostic test	31
Table 4.1	Comparison of display of arterial segments between IADSA And MRA by observer 1	35
Table 4.2	Comparison of visualization of ACOM, right PCOM and left PCOM between IADSA and MRA by observer 1	37
Table 4.3	Comparison of visualisation of A1, A2, M1 and P1 segments of The circle of Willis between IADSA and MRA by observer 2	39
Table 4.4	Comparison of visualisation of ACOM, right PCOM and left PCOM between IADSA and MRA by observer 2	41
Table 4.5	Display of arterial segments on MRA. Comparison between Observers 1 and 2	43
Table 4.6	Comparison of visualisation of ACOM, right PCOM and left PCOM on MRA by observers 1 and 2	45
Table 4.7	Sensitivity, specificity, predictive values and accuracy of 3D TOF MRA compared to IADSA in detection of the segments of the circle of Willis	47
Table 4.8	Measure of agreement between IADSA and 3D TOF MRA in Detecting the arterial segment of the circle of Willis by observer 1	48

Table 4.9	Measure of agreement between IADSA and 3D TOF MRA in Detecting the arterial segment of the circle of Willis by observer 2	49
Table 4.10	Measure of agreement between observers 1 and 2 in detection Of the arterial segments of the circle of Willis on 3D TOF MRA	50
Table 4.11	Morphology of the variants in the anterior part of the circle Of Willis	52

LIST OF FIGURES

Figure 1.1	Use of presaturation slab to suppress signal from venous blood	4
Figure 1.2	Schematic diagram of the vessels that form the circle of Willis	16
Figure 1.3	Anatomic variations in the anterior part of the Circle of Willis	18
Figure 1.4	Anatomic variations in the posterior part of the circle of Willis	19
Figure 3.1	Schematic diagram of the arterial circle of Willis	26
Figure 4.1	Comparison of depiction of (a) A1 segment (b) A2 segment (c) M1 segment and (d) P1 segment on IADSA and 3D TOF MRA by observer 1	36
Figure 4.2	Comparison between IADSA and 3D TOF MRA in depiction of (a) ACOM (b) Right PCOM and (c) left PCOM by observer 1	38
Figure 4.3	Comparison of depiction of (a) A1 segment (b) A2 segment (c) M1 segment and (d) P1 segment on IADSA and 3D TOF MRA by observer 2	40
Figure 4.4	Comparison of visualisation of (a) ACOM (b) right PCOM and (c) left PCOM between IADSA and 3D TOF MRA by observer 2	42
Figure 4.5	Comparison between observers 1 and 2 in depicting (a) A1 segment (b) A2 segment (c) M1 segment and (d) P1 segment of the circle of Willis on 3D TOF MRA	44

Figure 4.6	Comparison between observers 1 and 2 in depicting (a) ACOM Segment (b) right PCOM segment and (c) left PCOM segment Of the circle of Willis on 3D TOF MRA	46
Figure 4.7	MRA of the circle of Willis showing an example of variant a Of the anterior part of the circle where the ACOM segment is Present and example of variant a of the posterior part of the Circle where both the posterior communicating arteries are present. This is a complete circle of Willis	54
Figure 4.8	MRA of the circle of Willis showing an example of variant g of The anterior part of the circle where the ACOM is absent	55
Figure 4.9	MRA showed an arteriovenous malformation at the left Parasagittal region (a) which is confirmed by the left ICA run Of the IADSA study	56
Figure 4.10	Same patient as before, showing the arteriovenous malformation Lateral view on both MRA and IADSA	57
Figure 4.11	MRA of the circle of Willis showing splaying of the arterial Segments due to presence of a space occupying lesion. In Addition, there is narrowing of the left P1 and A1 segments Most likely secondary to the mass effect	58

ABBREVIATIONS

A1	A1 segment of anterior cerebral artery
A2	A2 segment of anterior cerebral artery
ACA	Anterior cerebral artery
ACOM	Anterior communicating artery
CTA	Computed tomographic angiography
IADSA	Intra-arterial digital subtraction angiography
M1	M1 segment of middle cerebral artery
MCA	Middle cerebral artery
MIP	Maximum intensity projection
MRI	Magnetic resonance angiography
P1	P1 segment of posterior cerebral artery
PCA	Phase contrast angiography
PCOM	Posterior communicating artery
3D TOF MRA	3 dimensional time of flight magnetic resonance angiography

ABSTRAK

Tajuk: Perbandingan diantara “3D TOF Magnetik resonance angiography” dan “intraarterial digital subtraction angiography” untuk pengimejan Circle of Willis.

Tujuan: Tujuan kajian ini dijalankan adalah untuk menguji ketepatan teknik “3D time of flight” magnetic resonans angiografi berbanding dengan teknik “intra-arterial digital subtraction” angiografi untuk pengimejan segmen-segmen arteri didalam “circle of Willis”.

Bahan-bahan dan Tatacara: Seramai 38 orang pesakit yang telah menjalani kedua-dua ujian “3D TOF MRA” dan “IADSA” di Hospital Universiti Sains Malaysia mulai November 1998 hingga Disember 2000 telah dimasukkan ke dalam kajian ini. Daripada jumlah ini, sebanyak 398 segmen-segmen arteri telah dibandingkan dan dianalisa. Dua orang pemerhati telah menjalankan analisis secara retrospektif terhadap imej-imej “IADSA” dan imej-imej “MIP” dari “3D TOF MRA” pada masa yang berlainan. Segmen-segmen A1, A2, M1 dan P1 telah dikategorikan sebagai normal, kecil atau tidak wujud, manakala segmen-segmen ACOM dan PCOM telah dikategorikan sebagai berfungsi, “patent” ataupun tidak kelihatan.

Keputusan: Teknik “3D TOF MRA” didapati bagus untuk mengesan segmen-segmen A1, A2, M1, P1 dan ACOM. Ia memberikan sensitiviti sebanyak 100%, 94.5%, 100%, 96.8% dan 100% untuk setiap segmen. Tiada kes positif palsu untuk segmen-segmen ini

dan nilai jangkauan positif adalah sebanyak 100%. Walau bagaimanapun, nilai jangkauan positif untuk segmen ACOM adalah sebanyak 89.5% dimana terdapat 2 kes positif palsu dari 19 segmen-segmen yang positif. Spesifisiti untuk segmen-segmen A1, A2 dan P1 amat memberansangkan iaitu sebanyak 100% dan bagus untuk segmen ACOM iaitu sebanyak 90.5%. Tiada kes-kes negatif palsu untuk segmen-segmen AI dan ACOM. Walau bagaimanapun, nilai jangkauan negatif untuk segmen-segmen A2 dan P1 adalah rendah, iaitu sebanyak 25% (3 daripada 4 keputusan adalah kes-kes negatif palsu). Teknik ini bagaimanapun adalah lemah untuk mengimej segmen PCOM dengan nilai sensitivity sebanyak 21.4% sahaja dan nilai jangkauan negatif hanya sebanyak 5.2%. Persetujuan untuk kedua-dua teknik “3D TOF MRA” dan “IADSA” berada didalam julat “perfect” dan “slight” untuk nilai-nilai kappa. Manakala persetujuan diantara kedua-kedua pemerhati mempunyai nilai kappa yang amat bagus untuk setiap segmen yang diimej menggunakan teknik “3D TOF MRA”.

KESIMPULAN: Persembahan “MIP” menggunakan teknik “3D TOF MRA” didapati sensitif untuk menunjukkan anatomi “circle of Willis” melainkan untuk segmen PCOM sahaja. Oleh kerana itu ia merupakan teknik yang boleh diharap sebagai teknik untuk mengimej segmen-segmen arteri ini.

ABSTRACT

TOPIC: Comparison between 3DTOF magnetic resonance angiography and intra-arterial digital subtraction angiography in imaging the circle of Willis.

AIM: The purpose of this study is to compare the accuracy of 3D time of flight magnetic resonance angiography (3D TOF MRA) with intraarterial digital subtraction angiography (IADSA) in depicting the arterial segments of the circle of Willis.

MATERIALS AND METHOD: 38 patients who had underwent both 3D TOF MRA and IADSA examinations in Hospital Universiti Sains Malaysia from November 1998 to December 2000 were included in this study giving a total of 398 arterial segments compared and analysed. Two observers performed blinded retrospective analysis of the IADSA images and MIP display of the 3D TOF MRA of the circle of Willis on separate sessions. The A1, A2, M1 and P1 segments were depicted as normal calibre, small or absent while the ACOM and PCOM segments were depicted as functional, patent or not visualised.

RESULTS: The 3D TOF MRA was good in depiction of the A1, A2, M1, P1 and ACOM segments of the circle of Willis with a sensitivity of 100%, 94.5%, 100%, 96.8% and 100% respectively. There were no false positive results for the A1, A2, M1 and P1 segments with a positive predictive values of 100%. However, the positive predictive value for the ACOM segment was 89.5% (2 false positive results out of 19 segments).

The specificity was excellent for the A1, A2 and P1 segments at 100% and acceptable for the ACOM segment at 90.5%. There were no false negative results for the A1 and ACOM segments. However, the negative predictive value for the A2 and P1 segments were low at 25% (3 out of 4 false negative results) and 60% (2 out of 5 false negative results) respectively. The 3D TOF MRA method was however a poor method for depiction of the PCOM segments with a sensitivity of 21.4%. The negative predictive value was very low at 5.2% with 53 out of 58 false negative results.

Observer agreement between IADSA and 3D TOF MRA range from kappa “perfect” to “slight” but inter-observer agreement for the 3D TOF MRA technique was excellent with the kappa values within the “perfect” range.

CONCLUSION: MIP display of the 3D TOF MRA is sensitive for depicting the anatomy of the circle of Willis except for the PCOM segment. It is thus a reliable method for screening of this arterial circle.

CHAPTER ONE

INTRODUCTION AND LITERATURE REVIEW

1.1 INTRODUCTION

Intra-arterial digital subtraction angiography (IADSA) is considered the gold standard in assessing the intracranial arteries. However, it is invasive and carries a small risk to the patient. In addition, it can be technically difficult, especially in the elderly and hypertensive patients where the arteries are often tortuous. In patients with certain conditions, such as those with allergic reaction to the contrast media, renal impairment etc. this investigation is also contraindicated, thus other techniques have been investigated in terms of feasibility in assessing the intracranial vasculature.

The 2 techniques that have been in used recently include magnetic resonance angiography (MRA) and computed tomographic angiography (CTA). MRA is a term used to describe a class of magnetic resonance imaging techniques designed to create angiographic images without the use of invasive techniques, contrast media or ionising radiation (Edelman et al., 1990; Rinck et al., 1993; Patruş et al., 1994; Sheppard, 1995). It also has the capacity to provide multiple projections of anatomically complex vascular abnormalities with a single data acquisition.

There are various techniques described for doing intracranial magnetic resonance angiography and the technique currently used in Hospital Universiti Sains Malaysia is 3D time of flight magnetic resonance angiography (3D TOF MRA).

The purpose of this study is to compare the accuracy of the magnetic resonance angiography with intra-arterial digital subtraction angiography in depicting the arterial segments of the circle of Willis.

1.2 Magnetic Resonance Angiography

1.2.1 Basic concept

There are two fundamental magnetic resonance acquisition techniques that are used in MRA. They are time of flight (TOF) and phase contrast angiography (PCA) (Sheppard, 1995). The TOF technique is based on the difference in signal intensity between static tissue and flowing blood while the PCA technique is based on the fact that flowing blood will interact with a special type of magnetic gradient (Sheppard, 1995).

In MRA, protons in the static tissue are referred to as static spins and protons in the blood as flowing spins. When placed in a magnetic field, the majority of these spins will line up in the direction of the magnetic field, forming what is called as longitudinal magnetization (Sheppard, 1995). To create an MR signal, energy in the form of a radio-frequency pulse is applied to force the longitudinal magnetization vector away from the equilibrium orientation and into the transverse plane. This pulse is called an excitation pulse (Sheppard, 1995). When the longitudinal vector is tilted into the transverse plane, the transverse magnetization vector is manifested. The magnitude of this excitation is called the flip angle and is measured in degrees of deflection away from the vertical orientation (Sheppard, 1995). It is governed by the pulse duration and amplitude.

Typically in an MRA examination, a flip angle from 20° to 80° is used depending on the vessels involved.

After the excitation, the magnetization vector will return to the original longitudinal orientation, releasing energy, which is detected as a signal called an echo, which forms the basis of the MR image. The process of returning the magnetization to the original longitudinal orientation is called relaxation (Sheppard, 1995). The magnetization relaxes by two mechanisms called T1 (longitudinal relaxation time) and T2 (transverse relaxation time). There is a direct relationship between the magnitude of the transverse magnetization and magnetic resonance signal intensity (Sheppard, 1995).

TOF MRA is the most widespread of all MR angiography methods. Jerome R. Singer first described this technique in 1959. It is also known as inflow or wash-in and wash-out technique (Rinck, 1993). There are two fundamental magnetic resonance acquisition techniques that are used in MRA. They are time of flight (TOF) and phase contrast angiography (PCA) (Sheppard, 1995). The TOF technique is based on the difference in signal intensity between static tissue and flowing blood while the PCA technique is based on the fact that flowing blood will interact with a special type of magnetic gradient (Sheppard, 1995).

The TOF technique has been widespread use in the study of the carotid arteries and the principal arteries of the brain.

The T1 (longitudinal relaxation) of blood and muscle is similar, i.e. approximately 800 to 950 milliseconds. If radio-frequency pulses are applied much faster than T1 ($TR \ll T1$) than both spins will saturate, thus the magnetization will be small and there will be very little MR signal detected (Sheppard, 1995). However, blood that has not been exposed to many radio-frequency excitations i.e. the unsaturated spins are constantly moving into the imaging slice. This causes the net magnetization of the flowing spins (blood) to be much larger than the static spins (tissue). In this way the contrast between flowing blood and static tissue is maximized (Sheppard, 1995).

To make the MRA useful, the arterial and the venous system need to be distinguished. Separation of the arterial from the venous flow is achieved by placing presaturation slabs on 1 side of the imaging slice or volume as depicted by figure 1.1 (Rinck, 1993; Sheppard, 1995).

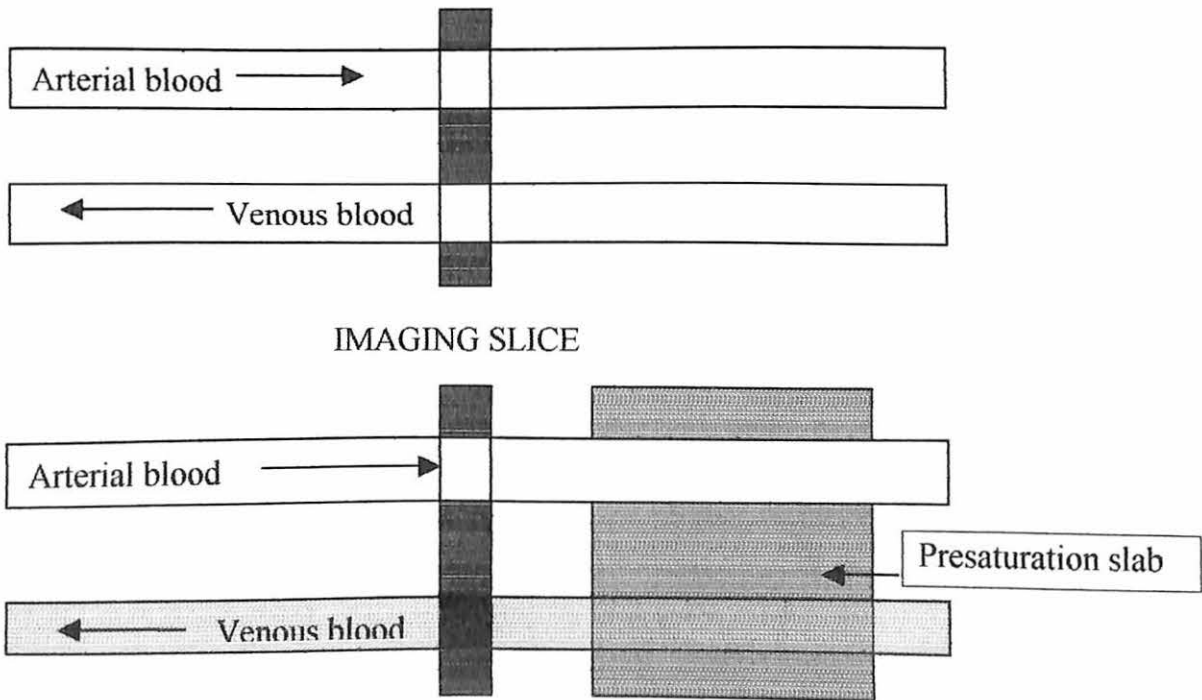


Figure 1.1: Use of presaturation slab to suppress signal from venous blood.

A presaturation slab applies many radio-frequency pulses to a discrete volume of tissue in a short period of time. All spins within that volume (static and flowing) will be magnetically saturated. As flowing spins leave the presaturation slab and enter a two dimensional (2D) imaging slice or three dimensional (3D) volume, they will generate no MR signal. Only flowing spins entering the imaging slice or volume from the opposite direction will be unsaturated and hence contribute an MR signal (Sheppard, 1995).

1.2.2 MR parameters and methods important in MRA acquisitions

- a) **Repetition time (TR)**. This determines the amount of saturation of static tissue. The shorter the repetition, the better the background suppression will be in the TOF technique. It also plays a major role in determining scan time. Typically, the shortest TR that a system will provide is utilized (Sheppard, 1995).
- b) **Echo time (TE)**. This plays an important role in the image quality of an MR angiography. As short an echo time is necessary because if the duration between the excitation and the echo is too long, intravoxel dephasing can cause significant signal loss. In addition, the T1 of fat is approximately 150 milliseconds, which is shorter than either blood or most of the static tissue. This means that fat can be difficult to saturate with repetition time and tip angle alone. Because the precession rate of water and fat are different, there are certain echo times in which the signal from fat is markedly reduced. At 1.5T a TE of 7 milliseconds is optimal for the best static tissue suppression and at 1.0T the optimal TE is 11 milliseconds (Sheppard, 1995).

- c) Tip angle. This determines how far the magnetization vector is rotated into the transverse plane. The larger the tip angle, the more static tissue is suppressed. For most arterial 2D acquisitions, a tip angle of 60 to 70 degrees is used. In the case of a 3D volume acquisition, the tip angle is usually much smaller. This is to control the effects of saturation of spins within the 3D volume. For most of the 3D acquisitions, a 20° to 30° tip angle is used in both the TOF and the PCA techniques (Sheppard, 1995).
- d) FOV. The size of the FOV affects the image quality, which is mostly signal to noise ratio and image resolution in MRA. It is important to consider the voxel size as the larger the voxel, the greater the partial volume effects will be. For small vessels, this will result in loss of the signal of the small vessels. Voxel is defined as $(FOV / M_{\text{frequency}}) \times (FOV / M_{\text{phase}}) \times (\text{slice thickness})$ where $M_{\text{frequency}}$ is the number of frequency encoding steps and M_{phase} is the number of the phase encoding steps. In general a voxel size that is smaller than the vessel of interest should be used. However, the disadvantage of using smaller voxel size is that it will lower the signal to noise ratio. But owing to the improve vessel detail, the contrast may be improved (Sheppard, 1995).
- e) Fixed and walking presaturation slabs. These are a series of slice selective radio-frequency pulses that are intended to saturate all spins within the slab. As mentioned earlier, the position of the presaturation slab is determined by whether the flow required in the MR angiogram is arterial or venous. The slab can be positioned parallel with the slices and set up to move with each 2D slice or 3D volume that is acquired. This is called a walking presaturation slab. A

presaturation slab can also be fixed in position so that it will not move with the 2D slices (Sheppard, 1995).

- f) Overlapping 3D volumes. The MOTSA technique (multiple overlapping thin slab acquisition) is used to overcome the limitation of slow flow saturation effect. 3D TOF is superior to 2D TOF in terms of resolution. However, owing to slow flow saturation effects, this results in significant loss of distal vessel detail. The MOTSA technique significantly reduces this problem by dividing the volume into multiple thin volumes. The spins do not have to cross as large a volume, hence saturation of slow flow is reduced. A problem with using multiple thin volumes is the production of venetian blind artifact. This is solved by overlapping the thin slabs as much as 30% to 50% (Sheppard, 1995).
- g) Magnetization transfer. This functions to improve static tissue suppression for TOF MRA study. In MR imaging there are 2 groups of water protons. They are free protons and those that are bound to macromolecules. The free protons have a narrow nuclear magnetic resonance spectrum (long T2 relaxation times) and these are the spins that are used to produce an MR image. The bound protons have a wide nuclear magnetic resonance spectrum (very short T2 relaxation times) and normally do not contribute to an MR image. In tissues that contain both pools of protons, there is a constant exchange of magnetization by a through space or dipole-dipole interaction. The magnetization between these pools is in a state of equilibrium. If the magnetization in either pool is saturated, there will be an effect on the magnetization of the other pool. The process of changing the magnetization of one pool to affect the other is the magnetization transfer. The tissues of interest

that are affected by magnetization transfer are muscles, gray and white matter and static blood. If the bound pool of protons is subjected to a saturation pulse, the magnetization transfer effect will cause the magnetization of free protons to be partly saturated as well. This results in a decrease in magnetization of the free protons with a net loss in signal intensity. If the magnetization effect is combined with a 2D or a 3D TOF acquisition for example in the brain, the gray and the white matter will have less signal due to the magnetization transfer effect. The brain will be darker and the signal intensity of the blood is minimally affected, thus increasing the contrast between static tissue and flowing blood (Sheppard, 1995).

1.2.3) Limitations of TOF

- a) TOF images suffer from problems with saturation of tortuous and slow flow and sometime poor background suppression, which degrades vessel conspicuity. Poor background suppression is especially apparent in the presence of short T1 species such as gadolinium enhancing lesions, fat and methaemoglobin (Rinck, 1993; Patruş et al., 1994; Sheppard, 1995).
- b) Compromise of image quality by patient movements. This is particularly problematic in patients who are prone to intrascan movement, including the elderly, demented and paediatric patients (Mc Gee et al., 2001). In their study Mc Gee and his colleagues tested a new class of algorithm, which has been shown, to correct for both translation and rotation induced artifacts. In this retrospective

technique, which is known as auto correction, no special pulse sequence is needed. It uses an image metric to measure changes in image quality induced by applying iterative phase correction estimates to the k-space data. In applying this method to MR angiography, the challenge is to improve image quality in larger data set i.e. 3D versus 2D with complex motion and lower signal to noise ratio values than other MR imaging examinations. The result of their study confirm that auto correction can improve the quality of 3D TOF MRA maximum intensity projection images that have been degraded by motion, and the auto correction did not adversely affect images without motion induced artifacts. A potential limitation to this technique is the long computation time of the algorithm and the restriction of the motion model to small rotations. Mc Gee et al. (2001) suggested that specific improvements that can be implemented to reduce computation time include performing auto correction on a faster computer system, using a multi processor array processor and optimizing the auto correction computer code.

1.2.4) Post processing of an MRA

With many MRA sequences it is possible to accumulate more than 100 images. This information can be reduced into the familiar form of an angiogram. This is most frequently accomplished with a *maximum intensity projection* (MIP) algorithm. The MIP algorithm will find the maximum intensity pixel along a specified projection line in all slices of an MR angiography data set. Then these maximum intensity pixels are copied onto the projection plane forming the angiographic image (Edelman et al., 1989; Rinck et

al., 1993; Sheppard, 1995). One disadvantage of MIP is that in routine clinical angiography bright non vascular tissues (e.g. fatty tissues) can represent highest signal intensity on the original pictures and thus be depicted on the angiogram. Such tissue can only be discriminated from vascular structures by their anatomy (Rinck et al., 1993).

1.2.5) Applications of intracranial 3D TOF MRA

This technique can be useful in the assessment of flow within the circle of Willis, diagnosis of cerebral aneurysms or arteriovenous malformations, diagnosis of ischaemic disease and as part of evaluation of intracranial neoplasm.

To be competitive with conventional angiography, MRA should not only show vessel morphology but should also provide functional information, such as delineation of specific vascular territories and the study of flow dynamics in the circle of Willis.

Several authors including Edelman et al. (1989), Patruş et al. (1994), Strotzer et al. (1998) and Nesbit et al. (1997) proposed that the determination of the direction of blood flow in the circle of Willis may be important in certain instances. These are in cases of cervical and intracranial vascular stenosis whereby the characterization of vascular supply and cross filling can play a part in determining stroke risk. Another application is in the pre-operative planning and post-operative evaluation of intracranial and extracranial anastomoses, ligations or endovascular occlusions. Demonstration of

patency and flow physiology can reduce the number of conventional angiogram needed in follow-ups of these patients.

In a study by Edelman et al. (1990), magnetic resonance angiography was applied to the study of blood flow dynamics in the circle of Willis. This was done by using selective presaturation of individual vessel. Presaturation causes signal loss within the territory supplied by the presaturated artery, without affecting vessels not crossing the presaturation slab. The authors claimed that the selective MR angiography technique is rapid and lengthens the study time for a routine MR examination by only a few minutes.

They found that MR accurately demonstrated the direction of blood flow, the presence or absence of collateral blood flow, and the blood supply to the pericallosal arteries and to the posterior cerebral arteries.

As mentioned earlier, collateral blood flow patterns may have significant clinical implications in patients at risk for stroke. The presence or absence of collateral blood flow, in association with cerebrovascular occlusive disease, may affect the clinical presentation and area of ischaemic damage. The combination of 3D MRA with the assessment of collateral blood flow by MR may prove useful in acute stroke patients. It can be used to show occlusion of portions of the circle of Willis due to an embolus or extension of a thrombus from the ICA and the presence of surviving collateral pathways (Edelman et al., 1990; Patruş et al., 1994).

MRA may also prove useful in patients with occipital lobe ischaemia. In patients with fetal posterior circulation, thrombosis or embolism of the ICA territory may cause ischaemic symptoms or infarction of the occipital pole. Conversely, such an anatomic configuration prevents occipital pole infarction in BA thrombosis (Edelman et al., 1990).

In another study by Nesbit and DeMarco (1997) demonstration of flow direction in the circle of Willis using 2D TOF MRA in association with concatenated (traveling) saturation bands were used instead of 3D TOF MRA. The advantage of this technique over the 3D TOF MRA method is that it has a relatively high sensitivity to slow flow due to minimization of spin saturation, thus there is improved demonstration of the vessels. It reveals flow at nearly full range of physiologic velocities. It fails to detect flow only at the extremes i.e. very slow flow or extremely fast flow such as in the jet of high grade stenosis. This allows visualization of most intracranial arteries and veins. This technique can provide important anatomic information and an overview of flow direction. However Nesbit and DeMarco (1997) found several disadvantages of this technique including difficulties in interpretation of overlapping vessels and confusion of arteries and veins; time constraint and disorientation due to the fact that only 1 direction of flow can be shown at a time by the 2D TOF technique.

The main advantage of presaturation is to facilitate understanding of the physiological flow through the arteries of the circle of Willis. On MRA 3 types of arteries can be identified, i.e. high flow or cross cerebral circulation, patent and non visualized arteries. Patency of the anterior or the posterior communicating artery is established when

the artery is visible and when the A1, A2, P1 and P2 segments had the same signal intensity. The anterior communicating artery is said to have high flow when A2 segments showed identical signal intensities with a single A1 segment while the contralateral A1 segment is absent or hardly visible. The posterior communicating artery is considered functional if it has the same diameter and signal intensity as the P2 segment while the P1 segment was hardly visible or absent (Patrux et al., 1994).

Failure to identify a communicating artery could be related to non-patency (atresia, thrombosis or spasm) or an absence of significant flow in baseline conditions (i.e. equilibrium between its 2 arterial feeders (Patrux et al., 1994). The study by Patrux et al. (1994) has demonstrated that in patent and non-visualized arteries, selective MRA did not offer additional information. Consequently, according to these authors, in the vast majority of cases, there is no need for such additional acquisitions, as a single acquisition is sufficient for portraying simultaneously the overall arterial supply and collateral flow around the circle of Willis.

The absence of any false positive MRA in their series validates MRA for assessment of patency of the circle of Willis when a vascular obstruction is suspected. Conversely, given the false negative results, non-visualization of an arterial segment by MRA may indicate contrast angiography (Patrux et al., 1994). There are thus 2 scenarios. In the first, all the arteries are shown by MRA, and the patency of the circle of Willis can be established. In the second, 1 or more arteries are not shown. After elimination of any technical fault, a study of the MRA projections must be complemented by examination of

the images of each slice, which can show a small slow flowing vessel excluded in the MIP reconstruction or, or by examination of the spin echo images which can display intraluminal flow void (Patrux et al., 1994). Once these problems have been clarified, the non-identification of an arterial segment can indicate congenital or acquired obstruction; very slow or nulled flow, owing to equivalent pressure conditions in the arteries on either side; or turbulent flow (Patrux et al., 1994).

As for the diagnosis of intracranial aneurysm, a study by Wilcock et al. (1996) showed that 3D TOF MRA is a sensitive and specific test for the detection and characterizations of aneurysms. They showed that the specificity of the technique was 100%; therefore they were confident that no unnecessary surgical procedures would have been performed on the basis of the MR images alone. In their study, they found that factors that could contribute to poor or non-visualization of aneurysms include significant local haematoma and motion artifact. Other studies by Horikoshi et al. (1994), Anzalone et al. (1995) and Adams et al. (2000) showed that the 3D TOF MRA technique is currently still inferior to IADSA in the pretreatment assessment of intracranial aneurysm and can miss small lesions i.e. those smaller than 3mm in diameter. However, Nesbit and DeMarco (1997) proposed that 3D TOF MRA can be important in the post-operative evaluation of intracranial and extracranial anastomoses, ligations or endovascular occlusions. According to them, demonstration of the patency and flow physiology can reduce the number of IADSA studies performed on these patients on follow-up evaluations. Identification of patients with vasospasm after acute subarachnoid haemorrhage is also possible with 3D TOF MRA (Grandin et al., 2000).

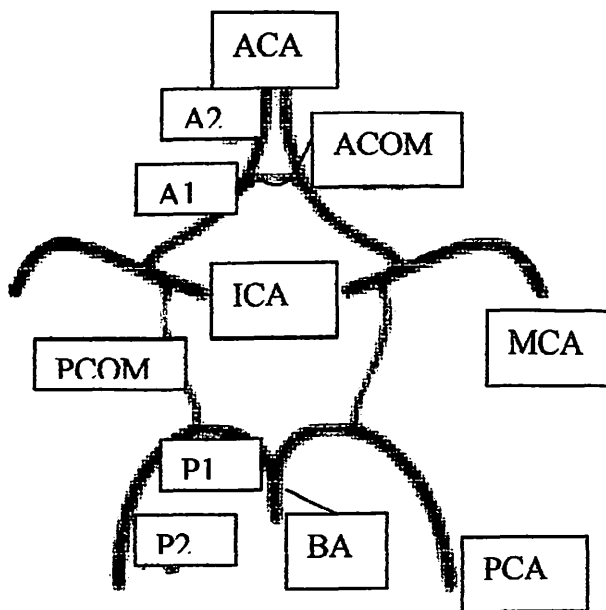
In cases of intracranial neoplasm, magnetic resonance angiography may be useful by providing information on their relationship to or displacement of adjacent intracranial arteries. Determination of direction of flow in the circle of Willis in addition will help in demonstrating vascular supply and drainage of the tumour (Nesbit and DeMarco, 1997).

1.3) Anatomic evaluation of the Circle of Willis

The circle of Willis, located at the base of the brain is a potential collateral pathway through which adequate distribution of cerebral blood flow can be maintained in case of impaired or decreased flow through one or more of its proximal feeding vessels. Johann Jacob Wepfer first studied it in 1658 and 6 years later in 1664, Sir Thomas Willis published his study on the circle of Willis (Lazorthes et al., 1979; Hartkamp et al., 1999).

Its ability to redistribute blood flow depends on its morphology: the presence and the size of the component vessels (Lazorthes et al., 1979; Hartkamp et al., 1998; Hartkamp et al., 1999). 3 supply channels, i.e. the 2 carotid arteries and the vertebrobasilar trunk and their anastomoses consisting of the anterior and the posterior communicating arteries, form the circle of Willis. It is a nine sided polygon with 3 anterior sides formed by the 2 anterior cerebral arteries and the anterior communicating artery; 2 anterolateral sides formed by the internal carotid arteries; 2 posterolateral sides formed by the posterior communicating arteries and the 2 posterior sides formed by the posterior cerebral arteries.

Figure 1.2: Schematic diagram of the vessels that form the circle of Willis.



In cadaveric studies performed by Lazorthes et al. (1979), he studied the constituent segments of the polygon including their length and diameter:

a) Anterior communicating artery:

The length of the artery varies from 0.1 to 4mm. Most frequently it is single but it can be double or triple. Sometimes it is not straight but v or y shaped if an artery of the corpus callosum arises from it. Its caliber appears to be inversely proportional to that of the anterior cerebral arteries. In general when the anterior cerebral arteries are thick, the communicating artery is reduced in size. Conversely when the anterior cerebral artery segment is hypoplastic in its

proximal segment, the communicating artery normally has a caliber equal to that of the opposite anterior cerebral artery. Its diameter varies between 0.1 to 2mm.

b) A1 segment of the anterior cerebral artery:

This runs anteromedially from its origin toward the midline where it meets the artery of the opposite side and anastomoses with it by means of the anterior communicating artery. On average, the length of this artery is 15mm and its diameter varies from 0.1 to 3mm. This artery is considered hypoplastic if it is less than 1mm.

c) Terminal segment of the internal carotid artery:

It has an average length of 10mm. Its diameter range from 1.5 to 5mm with a mean measurement of 2.5mm.

d) Posterior communicating artery:

This unites the internal carotid artery and the posterior cerebral artery. Its length varies between 5mm to 17mm and the average diameter is between 1mm to 2mm.

e) P1 segment of the posterior cerebral artery:

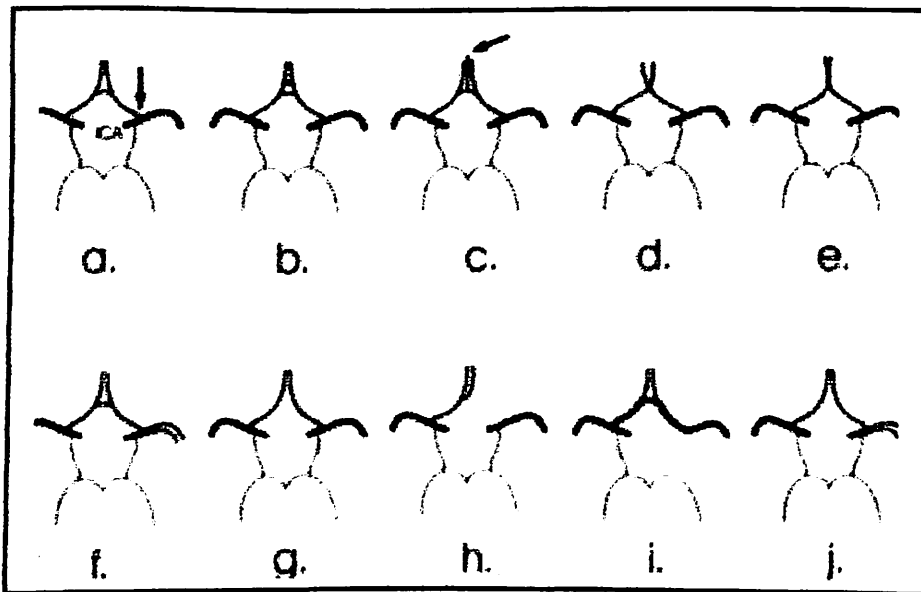
It runs obliquely lateralward and slightly forward from its origin to its union with the posterior communicating artery. Its length varies between 2mm to 15mm with an average length of 10mm. Its diameter is also variable between 0.1mm to 3mm. This vessel is considered hypoplastic if it is less than 1mm in diameter.

Lazorthes et al. (1979) classified the arterial segments into thin or thick where thin segments is defined as those with diameter less than 1mm. In their study of the adult cadaver, they found that the anterior communicating artery is thin in 27%, the A1

segment of the anterior cerebral artery is thin in 16%, the posterior communicating artery is thin on 1 side only in 20%, the posterior communicating artery is thin on both sides in 25%, the P1 segment of the posterior cerebral artery is thin on 1 side only in 16% and thin on both sides in 5%.

The circle demonstrates considerable morphologic variation among relatively healthy individuals, and authors of various studies have concluded that the anatomic variants play an important role in patients with carotid artery disease, although results varies (Edelman et al., 1990; Koh and Tan, 1993; Patruş et al., 1994; Stock et al., 1996; Hartkamp et al., 1998).

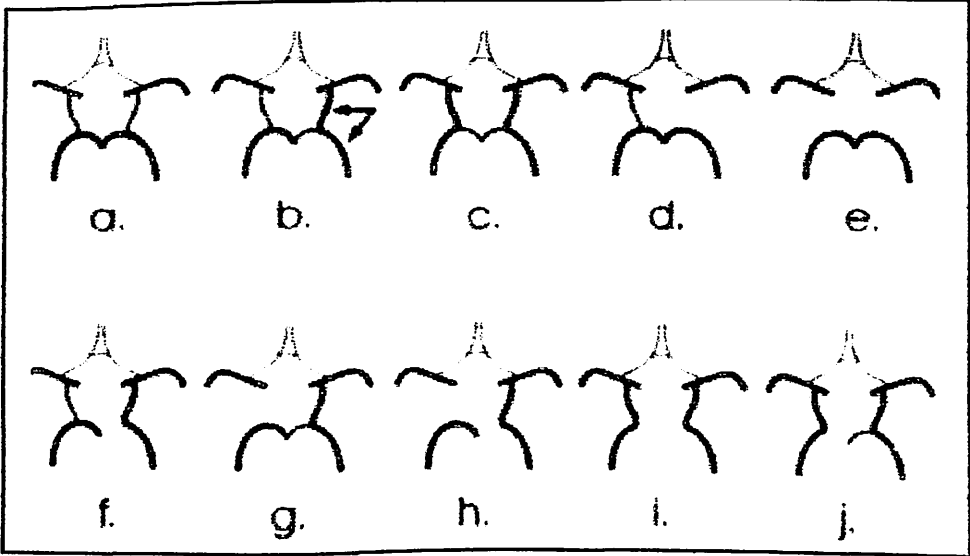
Figure 1.3: Anatomic variation in the anterior part of the circle of Willis.



Variants a to f are complete, whereas variants g to j are incomplete. In (a), the ACOM is single and the internal carotid artery bifurcates into A1 and M1 segment; in (b),

there are more than 1 of the anterior communicating artery; in (c), the medial artery of the corpus callosum arises from the anterior communicating artery; (d) there is fusion of the anterior communicating artery over a short distance; (e) the anterior cerebral artery arises from a common trunk and split distally into 2 post communicating segments; (f) the middle cerebral artery originates from the internal carotid artery as 2 separate trunks; (g) the anterior communicating artery is hypoplastic or absent; (h) 1 A1 segment is hypoplastic or absent, the other A1 segment gives rise to both A2 segments; (i) hypoplasia or absence of an internal carotid artery. The contralateral precommunicating segment of the anterior cerebral artery gives rise to both postcommunicating segment, which in turn gives rise to the ipsilateral middle cerebral artery; (j) hypoplasia or absence of an anterior communication. The middle cerebral artery arises as 2 separate trunks (Hartkamp et al., 1998, Hartkamp et al., 1999)

Figure 1.4: Anatomic variations in the posterior part of the circle of Willis.



Variants a to c are complete while variants d to j are incomplete. In (a), both posterior communicating arteries are present; (b) posterior cerebral artery originates predominantly from the internal carotid artery. This variant is known as a unilateral fetal type posterior cerebral artery (arrows). The posterior communicating artery on the contralateral type is patent; (c) bilateral fetal type posterior cerebral arteries with both precommunicating segments of the posterior cerebral arteries patent; (d) unilateral posterior communicating artery present; (e) hypoplasia or absence of both posterior communicating arteries and isolation of the anterior and posterior parts of the circle at this level; (f) unilateral fetal type posterior cerebral artery and hypoplasia or absence of the precommunicating segment of the posterior cerebral artery; (g) unilateral fetal type posterior cerebral artery and hypoplasia or absence of the contralateral posterior communicating artery; (h) unilateral fetal type posterior cerebral artery and hypoplasia or absence of both a precommunicating segment of the posterior cerebral artery and the posterior communicating artery; (i) bilateral fetal type posterior cerebral arteries with hypoplasia or absence of both precommunicating segments of the posterior cerebral arteries; (j) bilateral fetal type posterior cerebral arteries with hypoplasia or absence of 1 precommunicating segment of a posterior cerebral artery (Hartkamp et al., 1998, Hartkamp et al., 1999).

The lower limit of normal vessel diameter is arbitrary and affects the number of vessel segments classified as hypoplastic, which also affects the prevalence of circles defined as complete. Hartkamp et al. (1998) used a diameter of 1mm as the lower limit for normal diameter for the vessels of the circle of Willis. Stock et al. (1996) also used a

diameter of 1mm as the lower limit of normal claiming that clinically only collaterals with at least this diameter are able to prevent watershed infarction.

CHAPTER TWO

AIM AND OBJECTIVES

2) AIM AND OBJECTIVES

2.1) AIM

To compare 3D time of flight magnetic resonance angiography (3D TOF MRA) with intraarterial digital subtraction angiography (IADSA) in depicting the arterial segments of the circle of Willis.

2.2) OBJECTIVES

- a) To determine the sensitivity, specificity and the predictive values of 3D TOF MRA in identifying the arterial segments of the circle of Willis.
- b) To evaluate whether the patency and the functionality of the anterior communicating and the posterior communicating arteries can be determined by 3D TOF MRA technique.
- c) To compare the agreement between the 2 techniques in depicting the arterial segments of the circle of Willis.
- d) To compare between 2 observers: 1) a radiology trainee and 2) a consultant radiologist in depiction of the arterial segments of the circle of Willis on 3D TOF MRA technique. This is to determine whether level of experience plays a part in correct reading of the MIP reconstructed images.
- e) To evaluate the 3D TOF MRA technique in identifying variants of the vessels in the arterial circle of Willis.
- f) To evaluate the 3D TOF MRA technique in identifying pathological changes of the segments of the arterial circle of Willis.

2.4) NULL HYPOTHESIS:

There is no significant difference between 3D TOF MRA and IADSA in depicting the arterial segments of the circle of Willis.

CHAPTER THREE

METHODOLOGY

3) METHODOLOGY

This study was conducted as a combination of retrospective and prospective study. The data collection was done from September 1999 to January 2001. The study population was taken from all patients of any age who underwent both magnetic resonance imaging (MRI) of the brain with 3D time of flight magnetic resonance angiography (3D TOF MRA) of the circle of Willis and cerebral angiography (intraarterial digital subtraction angiography, IADSA).

The duration between these two studies was taken to be not more than 1 month apart. There was no actual figure in the literature to suggest the maximum time between these 2 techniques. Taking into account the possibilities of pathological process of the vessels itself, or pathological process within the vicinity of the vessels which could alter the appearance of the vessels, it was decided that the duration between these 2 techniques should not be more than 1 month apart to prevent differences in the depiction of the arterial segments due to the progression of the patients' disease process.

A total of 54 patients underwent both intraarterial digital subtraction angiography study and 3D TOF MRA study, from November 1998 until December 2000, however only 38 patients were included in this study. Among the 16 cases not included, 11 were because the duration was too far apart, i.e. more than 1 month; 2 cases were due to loss of images (data was not archived) and 3 cases were due to poor MRA images which were not of diagnostic quality. Majority of the patients were Malay (34 patients), followed by 3

Chinese and 1 Siamese patient. The gender distribution was almost equal with 20 male (53%) and 18 female (47%) patients with the patients' age ranging from 7 to 71 years old with mean age of 37.4 years. The largest age group being those in the 5th decade, making up 31.6% (12 / 38) from the total patient population.

All patients were from Hospital Universiti Sains Malaysia, Kubang Kerian, Kelantan. The patients were identified from the Department of Radiology computerised database. Two observers consisting of the author herself (observer 1) and a consultant radiologist (observer 2) performed retrospective analysis of the 3D TOF MRA and IADSA images of the circle of Willis. The observers were blinded to the clinical information about the patients. The image analysis of these two different techniques for each patient was done on two separate sessions so as to prevent bias in the interpretation. Observer 1 analysed the images for both techniques first, followed by analysis by observer 2. During the image analysis by observer 2, observer 1 was present so that any discrepancies were discussed and the final result from observer 2 on the 3D TOF MRA technique was used in the statistical analysis for the accuracy of this technique.

3.1) IMAGING MODALITIES

- 1) For the 3D TOF MRA, studies were performed with a 1.0T strength Signa Horizon LX GE Medical Systems equipment. The parameters used were:
 - a) 31 / 4 (repetition time, TR in milliseconds / echo time, TE in milliseconds).
 - b) 20° flip angle.